IBRO Neuroscience
Research Article

Effects of GABAergic and glutamatergic inputs on temporal prediction signals in the primate cerebellar nucleus

Akiko Uematsu[1,2] and Masaki Tanaka[1]

[1]Department of Physiology, Hokkaido University School of Medicine, Sapporo 060-8638, Japan
[2]Department of System Neuroscience, National Institute for Physiological Sciences, Okazaki 444-8585, Japan

Text pages: 23
Figures: 4
Table: 0

Abstract: 246 words

Correspondence to:

Masaki Tanaka, PhD, MD
Department of Physiology
Hokkaido University School of Medicine
North 15, West 7, Sapporo 060-8638, Japan
Tel: +81 11-706-5039, Fax: +81 11-706-5041
E-mail: masaki@med.hokudai.ac.jp

Highlights

- Neurons in the cerebellar nuclei show entrained activity to repetitive visual stimuli
- Periodic predictive activity appears to be mostly regulated by GABAergic input
- Balance between GABAergic and glutamatergic signals determines baseline activity
- Blockade of GABAergic input decreases neuronal variation
- Cerebellar output is shaped by the interplay of GABAergic and glutamatergic signals

Abstract

The cerebellum has been shown to be involved in temporal information processing. We recently demonstrated that neurons in the cerebellar dentate nucleus exhibited periodic activity predicting stimulus timing when monkeys attempted to detect a single omission of isochronous repetitive visual stimulus. In this study, we assessed the relative contribution of signals from Purkinje cells and mossy and climbing fibers to the periodic activity by comparing single neuronal firing before and during local infusion of GABA or glutamate receptor antagonists (gabazine or a mixture of NBQX and CPP). Gabazine application reduced the magnitude of periodic activity and increased the baseline firing rate in most neurons. In contrast, during the blockade of glutamate receptors, both the magnitude of periodic firing modulation and the baseline activity remained unchanged in the population, while a minority of neurons significantly altered their activity. Furthermore, the amounts of changes in the baseline activity and the magnitude of periodic activity were inversely correlated in the gabazine experiments but not in the NBQX+CPP experiments. We also found that the variation of baseline activity decreased during gabazine application but sometimes increased during the blockade of glutamate receptors. These changes were not observed during prolonged recording without drug administration. These results suggest that the predictive neuronal activity in the dentate nucleus may mainly attribute to the inputs from the cerebellar cortex, while the signals from both mossy fibers and Purkinje cells may play a role in setting the level and variance of baseline activity during the task.

Keywords: sensory prediction, deep cerebellar nucleus, Purkinje cell, mossy fiber, monkey

Abbreviations: CPP, (±)-3-(2-carboxypiperazin-4-yl)-propyl-1-phosphonic acid; NBQX, 1,2,3,4-Tetrahydro-6-nitro-2,3-dioxo-benzo[f]quinoxaline-7-sulfonamide hydrate

Introduction

In motor control, the cerebellum coordinates the timing of contractions of individual muscles and helps the cerebral cortex generate strong driving signals for movement initiation (Thach et al., 1992; Nashef et al., 2019). It is also believed that the cerebellum forms forward models that allow for predictive motor control and generate prediction error signals for learning (Wolpert et al., 1998; Shadmehr, 2017). Although neurons in the output node of the cerebellum—the cerebellar nuclei—often exhibit a transient activity during movements (Harvey et al., 1979; Fortier et al., 1989), its generation mechanism remains uncertain. In addition to neuromodulatory signals originated from the raphe nuclei and the locus coeruleus, the cerebellar nuclei receive drive signals from two different sources: glutamatergic input via mossy and climbing fibers from the brainstem, and GABAergic input from Purkinje cells in the cerebellar cortex. A possible mechanism for the generation of the movement-related transient activity in the nucleus is the direct excitation from the brainstem (Holdefer et al., 2005). Other possible mechanisms are either disinhibition from sustained inhibitory inputs from the cerebellar cortex (van Kan et al., 1993; Steuber et al., 2011; Heiney et al., 2014; Ishikawa et al., 2014; Chabrol et al., 2019), or post-inhibitory rebound following transient inhibition that has been observed in cerebellar slices (Aizenman and Linden, 1999; Person and Raman, 2012), although the role of the latter in behaving animals is controversial (Alviña et al., 2008). It has also been proposed that the synchronous activity of Purkinje cells may play a role (Person and Raman, 2012; Tang et al., 2019).

Besides movement execution, the cerebellum is also known to be involved in motor planning and relevant cognitive functions (Bellebaum et al., 2012; Koziol et al., 2014; Sokolov et al., 2017; Tanaka et al., 2021). Anatomical studies have indicated a close link between the lateral cerebellum and the association areas in the cerebral cortex (Ramnani, 2006; Strick et al., 2009), and functional imaging studies have shown that the cerebellum is strongly activated during a variety of cognitive tasks (Stoodley and Schmahmann, 2009; E et al., 2014). In particular, recent studies suggest that the cerebellum plays a role in temporal information processing, regardless of the execution of movement (Ivry et al., 1988; Sakai et al., 1999; Teki and Griffiths, 2016; Breska and Ivry, 2020). In fact, subjects with cerebellar damage have been shown to have difficulty in initiating movements at the correct time (Perrett et al., 1993; Spencer et al., 2003; Bares et al., 2011; Matsuda et al., 2015; Breska and Ivry, 2016) and in predicting the timing of future sensory events (Roth et al., 2013).

Recently, the neuronal mechanisms underlying temporal information processing in the cerebellum have been investigated using experimental animals trained to monitor elapsed time

(Ashmore and Sommer, 2013; Ohmae et al., 2017) and predict the timing of stimulus appearance (Cerminara et al., 2009). Our recent studies also demonstrated that neurons in the cerebellar dentate nucleus exhibited periodic activity predicting stimulus timing when monkeys attempted to detect an omission of repetitive visual stimulus (Ohmae et al., 2013; Uematsu et al., 2017). Since neural activity synchronized to periodic events has been reported in the cerebellum (Fujioka et al., 2012; Kotz et al., 2014), the basal ganglia (Merchant et al., 2011; Hove et al., 2013; Kameda et al., 2019), the motor thalamus (Matsuyama and Tanaka, 2021) and the cerebral cortex (Bartolo and Merchant, 2009; Comstok et al., 2021), the temporally specific signals found in the deep cerebellar nuclei may reflect external signals transmitted via mossy fibers or might be generated within the cerebellar cortex.

To examine these possibilities, we pharmacologically manipulated the glutamatergic and GABAergic inputs during single neuronal recordings from the cerebellar dentate nuclei in behaving monkeys. We found that local application of a $GABA_A$ receptor antagonist decreased the magnitude of periodic activity during sensory prediction and increased the baseline firing rate, while the effects of glutamate receptor antagonists were inconsistent and smaller. These results suggest that the predictive periodic activity in the cerebellar nucleus is shaped by the interplay between the inputs from the cerebellar cortex and the brainstem, while the former may play a dominant role. These inputs may also cooperatively regulate the level and variance of baseline activity in the dentate nucleus.

Experimental procedures

Animal preparation

Three Japanese monkeys (*Macaca fuscata*, 6–9 kg, one female and two males, monkeys A, H and Z) were used. All experimental protocols were evaluated and approved by the Hokkaido University Animal Care and Use Committee and were in accordance with the Guidelines for Proper Conduct of Animal Experiments (Science Council of Japan, 2006). After the animals were trained to voluntarily sit in the primate chair, a pair of head holders and an eye coil were implanted in separate surgeries under general isoflurane anesthesia using the same procedures described in previous studies in our laboratory (Tanaka, 2005). Analgesics were administered during each surgery and the following few days. After full recovery from the surgery, the animals were further trained on behavioral tasks with their heads restrained to the primate chair. Horizontal and vertical eye position were recorded using the search coil technique (MEL-25, Enzanshi Kogyo). After several months of training, a recording chamber was placed above the burr hole centered 6–8 mm posterior to the interaural line to allow vertical electrode penetration

targeting the cerebellum. The chamber location with respect to the deep cerebellar nuclei was verified using magnetic resonance imaging (MRI).

Visual stimuli and behavioral tasks

Experiments were controlled by a Windows-based stimulus presentation and data acquisition system (TEMPO, Reflective Computing). Visual stimuli were presented on either a 24-inch cathode ray tube monitor (refresh rate, 60 Hz; GDM-FW900, Sony) or a 27-inch liquid crystal display (refresh rate: 144 Hz; XL2720Z, BenQ) that were placed in a darkened booth. The monitors were located 38 or 40 cm away from the eyes and subtended 64 × 44° (Sony) or 73 × 45° (BenQ) of visual angle.

We used the missing oddball paradigm developed previously (Ohmae et al., 2013; Uematsu et al., 2017). In this task (Fig. 1A), each trial began with the appearance of a central fixation point (FP, red 0.5° square). After eye fixation, a saccade target (gray 1.0° square) appeared either 16° left or right of the FP. During the maintenance of fixation, a brief visual stimulus (white unfilled 2° square, 35 ms in duration) surrounding the FP was repeatedly presented at a fixed interstimulus interval (ISI) of either 150 or 400 ms. After a random 2000–4800 ms period, one of the repetitive stimulus was omitted (missing oddball). To receive a juice reward, the animals were required to make a saccade to the target in response to the stimulus omission within 600 ms. A previous study in humans has shown that the detection of stimulus omission with an ISI longer than 250 ms relies on temporal prediction, while that for a shorter ISI relies on the low-level temporal grouping of sensory events (Ohmae and Tanaka, 2016).

Physiological procedures during local drug injection

We recorded from single neurons in the posterior part of the dentate nucleus before and during drug infusion at the recording site using a homemade injectrode consisting of a tungsten microelectrode (shank diameter 150 μm, FHC Inc.) and a silica tube (105 μm o.d., Polymicro Technologies Inc.; Tachibana et al., 2008; Chiken and Nambu, 2013). The distance from the opening of the injection tube to the electrode tip was 600–750 μm, which was within the effective radius of drugs delivered using this technique (Kita et al., 2004). The location of injectrode penetration was adjusted using a grid (Crist Instruments) attached to the recording chamber. The injectrode was inserted into the brain through a 23-gauge stainless steel tube and was advanced remotely using a micromanipulator (MO-97S, Narishige). We searched for neurons exhibiting the task-related firing modulation, as described in detail previously (Ohmae et al., 2013). Briefly, these neurons exhibited an oscillatory activity in response to repetitive visual stimuli with the peak activity around the time of each stimulus (Figs. 2A and C). Signals

obtained from the electrodes were amplified, filtered (300 Hz–10 kHz), sampled at 50 kHz, and analyzed online using a spike sorter with a template-matching algorithm (ASD, Alpha Omega Engineering) to isolate single neurons.

Once a task-related neuron was isolated, we collected the pre-injection control data for more than 10 trials for each condition (ranging from 11–46 trials, mean ± SD, 24.8 ± 6.9, n = 51; n = 18, 17, and 16 for monkeys A, H, and Z, respectively). Thereafter, we attempted to locally infuse drugs while the same single neuron remained isolated. The silica tube composing the injectrode was connected to a 10-μL Hamilton microsyringe that contained either 6-Imino-3-(4-methoxyphenyl)-1(6H)-pyridazinebutanoic acid hydrobromide (gabazine; Sigma-Aldrich and Tocris-Bioscience, 1–5 mM dissolved in saline) or a mixture of (±)-3-(2-carboxypiperazin-4-yl)-propyl-1-phosphonic acid (CPP, Sigma-Aldrich, 0.5 mM) and 1,2,3,4-Tetrahydro-6-nitro-2,3-dioxo-benzo[f]quinoxaline-7-sulfonamide hydrate (NBQX, Sigma Aldrich, 0.5 mM). Gabazine, CPP, and NBQX are $GABA_A$, NMDA, and AMPA receptor antagonists, respectively. These drugs were pressure injected remotely at a rate of 5–15 nL/min using a micropump (Nanojet CXY-1, Chemyx Inc.). Total injection volume at each site was typically 0.1–0.4 μL. In some experiments we maintained a negative pressure during the initial pre-injection recording to avoid drug leakage that could cause underestimation of drug effects. Specifically, among 28 neurons examined quantitively, baseline activity (500 ms before the stimulus presentation, see below) measured in the first and second half of pre-injection trials was significantly different for only five neurons (unpaired t test, $p < 0.05$).

Data acquisition and analysis

The eye movement data and the timing of each spike were sampled at 1 kHz, and were saved in files during experiments. Data were analyzed offline using Matlab (Mathworks). We included data from neurons that exhibited significant firing modulation in response to each repetitive stimulus and were tested for at least twelve trials in each condition during drug application (ranging from 12–100 trials, mean ± SD, 43.7 ± 27.9, n = 28; gabazine, n = 9, 5 and 1, CPP + NBQX, n = 2, 3 and 8 for monkeys A, H and Z, respectively). After each experiment, we moved the plunger of the Hamilton syringe and visually checked if any drug solution was released from the injectrode. Data were discarded if we failed to confirm drug ejection and did not find any change in neuronal activity during drug infusion. For each neuron, the spike waveforms before and during drug infusion were saved online at 50 kHz using the spike sorting system (ASD, Alpha Omega Engineering).

To analyze data, each experiment from the three monkeys was treated as an independent

variable and a fixed-effect model was used. For the quantitative analyses, the data obtained just before drug infusion were compared with those obtained > 4 min after the start of drug infusion. To examine the time courses of neuronal activity, we computed spike density by convolving a Gaussian kernel (σ = 30 ms) to the millisecond-to-millisecond mean firing rate for each condition. The effects of each drug were assessed by comparing the spike densities during 400–2000 ms from the first stimulus in the sequence in trials with a 400-ms ISI. This interval was chosen because the stimulus omission occurred at or later than 2000 ms from the first stimulus and therefore the alignment of the data at the time of stimulus omission results in a mixture of trials with different number of stimulus repetition that can change the size of firing modulation (Ohmae et al., 2013). To quantify the changes in baseline activity and the task-related firing modulation simultaneously, we performed a regression analysis on the pair of data obtained before and during drug infusion, calculating the shift (offset) and gain (slope) components for each experiment. The regression analysis allowed us to properly evaluate the changes in neuronal activity without any bias resulting from the selection of measurement interval within each ISI. We also measured baseline activity during 500 ms before the first stimulus onset (baseline period).

To test for statistical differences, a two-tailed *t* test was used for normally distributed samples (Lilliefors test, $p > 0.01$), and the nonparametric Wilcoxon rank sum test was used otherwise. When comparing data between different drug conditions, the Welch's method was used, which is applicable to non-equivariate data samples. For statistical evaluation of the shift and gain components in individual neurons, we computed bootstrap 95% confidence intervals for each value (1000 iterations) and reported the number of neurons showing a significant difference from zero (shift component) or unity (gain component) in the Results.

Histological procedures

The recoding sites in monkey Z were reconstructed from histological sections (Fig. 1B). After completion of the experiments, several marking lesions were made by passing direct current (tip negative, 10–20 μA for ~1 min, 800–1000 μC) through the electrodes. After sedation with midazolam and medetomidine, the animal was deeply anesthetized with pentobarbital sodium (> 60 mg/kg, i.p.). Several landmark pins were inserted using the grid system. The monkey was then perfused transcardially with 0.1 mM phosphate buffered saline followed by 4% paraformaldehyde. The brain was removed, fixated overnight, blocked, and equilibrated with 40% sucrose. Coronal sections (50 μm thick) were cut on a freezing microtome, and histological sections were stained with cresyl violet.

Results

Effects of GABA receptor antagonist

Figure 2A compares the activity of a representative neuron before and during infusion of a $GABA_A$ receptor antagonist (gabazine) in the missing oddball task (400-ms ISI). During gabazine administration, the baseline firing rate measured during 500 ms before the start of stimulus sequence (Fig. 2A, left panel) greatly increased from 92.1 ± 18.0 spikes/s to 133.8 ± 9.1 spikes/s (mean ± SD, Welch's t test, $t_{27.0} = -8.97$, $p < 10^{-8}$), while the magnitude of firing modulation for each repetitive stimulus slightly decreased. When we computed the gain and shift components, the values were 0.78 (bootstrap 95% CI [0.61, 0.91]) and 67.5 ([53.7, 87.3]), respectively ($r^2 = 0.92$). Although the sample spike waveforms (Fig. 2B) slightly changed during gabazine application, the neuron remained well isolated throughout the recording period. On the other hand, saccadic reaction time did not change significantly during drug application (202 ± 36 ms versus 213 ± 56 ms, mean ± SD, Wilcoxon rank sum test, $Z = -0.29$, $p = 0.77$), likely because the amount of drug infusion was small (approximately 100 nL for this example). Similar results were also obtained from the other two example neurons shown in Figure 2C. The gain and shift components of the neuron in the left panel were 0.61 ([0.41, 0.73]) and 106.2 ([93.4, 126.2]), respectively ($r^2 = 0.75$). Those in the right panel were 0.60 ([0.35, 0.70]) and 22.1 ([14.2, 41.0]), respectively ($r^2 = 0.67$).

Figure 3A summarizes the data from fifteen gabazine experiments (red circles). When gabazine was administered, the magnitude of firing modulation for each repetitive stimulus generally decreased, and the mean of the gain component was significantly less than unity (mean ± SD, 0.82 ± 0.23, $n = 15$, one-sample t test, $t_{14} = -2.98$, $p = 0.0099$). According to the bootstrap analysis for individual neurons (Experimental procedures), nine out of 15 neurons showed a significant decrease in the magnitude of the oscillatory activity (Fig. 3C, filled red bars).

In contrast, the baseline firing rate measured before the stimulus presentation increased significantly (mean ± SD, 59.4 ± 24.2 spikes/s and 73.8± 35.3 spikes/s for the trials before and during gabazine application, respectively; paired t test, $t_{14} = -2.30$, $p = 0.037$). Likewise, the shift component computed from the time course of neuronal activity during 400–2000 ms after the first stimulus averaged 23.4 ± 34.1 (SD) and was significantly greater than zero (one-sample t test, $t_{14} = 2.66$, $p = 0.019$). For individual neurons, the shift component was significantly greater than zero for 11 out of 15 neurons (bootstrap, $p < 0.05$) and no neuron showed a significant decrement of the value. Changes in the baseline activity measured before the

stimulus presentation correlated with the shift component calculated for the activity during stimulus repetition (Spearman's rank correlation coefficient, $rho = 0.87$, $p < 10^{-15}$, Fig. 3B), although the former tended to be smaller than the latter (paired t test, $t_{14} = -2.19$, $p = 0.046$).

The shift component and the gain component inversely correlated (Spearman's rank correlation coefficient, $rho = -0.68$, $p = 0.0065$), indicating that these changes were linked with each other and likely resulted from specific pharmacological effects. On the other hand, we failed to find any significant correlation between dosage (concentration × injection volume) and each component (Spearman's rank correlation coefficient, gain component: $rho = -0.12$, $p = 0.66$, shift component: $rho = 0.42$, $p = 0.15$).

During gabazine administration, neuronal activity immediately after stimulus omission (measured during 200 ms) increased significantly in seven of fifteen neurons (unpaired t test, $p < 0.05$) but not in the population as a whole (76.6 ± 46.9 spikes/s versus 91.8 ± 57.9 spikes/s, paired t test, $t_{14} = -2.07$, $p = 0.06$). These changes in individual neurons were mostly due to the increased activity for each repetitive stimulus, rather than due to the enhancement of the response to stimulus omission. When the firing modulation for the stimulus omission was measured by subtracting the activity around the time of the preceding stimulus (± 50 ms), only one neuron showed a significant drug effect (unpaired t test, $p < 0.05$) but not in the population (4.6 ± 18.3 spikes/s versus 5.5 ± 17.4 spikes/s, paired t test, $t_{14} = -0.64$, $p = 0.53$).

Overall, reaction time did not change significantly during gabazine application (mean ± SD, 285 ± 74 ms versus 287 ± 72 ms, paired t test, $t_{14} = -0.24$, $p = 0.81$). In individual experiments, only one out of 15 experiments revealed a significant difference in reaction time during drug infusion (Wilcoxon rank sum test, $Z = -3.11$, $p < 0.05$).

We also found that gabazine reduced the variance of baseline neuronal activity. Figure 3D compares the coefficient of variation (CV) of inter-spike intervals during the baseline period (500 ms before the first stimulus) between the trials before and during drug infusion. In the population, the CV significantly decreased during gabazine application (mean ± SD, 0.83 ± 0.25 versus 0.69 ± 0.25, paired t test, $t_{14} = 2.49$, $p = 0.026$). For individual neurons, the CV changed significantly in eleven out of 15 neurons (9 decreased and 2 increased, one-tailed F test, $p < 0.01$). In contrast, we did not find any significant change in the width of individual spikes during experiments (paired t test, $t_{14} = -1.16$, $p = 0.27$).

Effects of glutamate receptor antagonists

Figure 2D illustrates the activity of a representative neuron before and during administration of glutamate receptor antagonists (a mixture of CPP and NBQX, Experimental procedures).

Following infusion of CPP + NBQX compound, the baseline activity 500 ms before the stimulus presentation slightly but significantly decreased from 49.1 ± 9.8 spikes/s to 41.5 ± 12.0 spikes/s (mean ± SD, Welch's *t* test, $t_{39.0} = 2.28$, $p = 0.028$). The gain and shift components computed during the stimulus repetition were 1.05 (95% CI [0.71, 1.19]) and −11.98 ([−19.61, 8.24]), respectively ($r^2 = 0.93$), indicating that this neuron only exhibited a change in the level of activity without change in the magnitude of periodic activity. The neuron remained well isolated throughout the recording period, and the spike waveforms during drug infusion were similar to those before injection (Fig. 2E). The other two example neurons shown in Figure 2F exhibited the gain component of 0.96 (95% CI [0.65, 1.14], $r^2 = 0.86$, left panel) and 1.38 ([1.05, 1.63], $r^2 = 0.84$, right), and the shift component of −13.05 ([−22.11, −1.37], left) and −35.53 ([−49.30, −16.36], right).

Figure 3A shows the data from thirteen CPP + NBQX sessions (blue triangles). In the population, both the gain and shift components remained unchanged during drug infusion (gain: 0.95 ± 0.15, one-sample *t* test, $t_{12} = -1.26$, $p = 0.23$; shift: 2.5 ± 19.8, $t_{12} = 0.45$, $p = 0.66$). For individual neurons, eight out of 13 neurons exhibited a significant change in the baseline activity measured before the stimulus onset (3 increased and 5 decreased, Welch's *t* test, $p < 0.05$). A significant change in the gain component was found in four neurons (Fig. 3C, filled blue bars, bootstrap, $p < 0.05$), while the baseline value significantly altered in five neurons (either increase or decrease).

We found that these two components did not correlate significantly (Spearman's rank correlation coefficient, $rho = -0.47$, $p = 0.11$). Thus, although the glutamatergic inputs might contribute to both the adjustment of the level of baseline activity and the magnitude of periodic activity for each repetitive stimulus, these effects varied from neuron to neuron. This was in contrast to the fact that the blockade of GABAergic inputs decreased the periodic activity (Fig. 3C) and increased the baseline firing rate (Fig. 3B) in most neurons.

In all 13 experiments, we failed to detect any significant change in the saccadic reaction time during drug infusion (Wilcoxon rank sum test, $p > 0.05$). There was no significant correlation between dosage and each component (Spearman's rank correlation coefficient, gain component: $rho = 0.42$, $p = 0.15$, shift component: $rho = 0.10$, $p = 0.76$). We found that the blockade of glutamate receptors significantly changed the activity immediately after stimulus omission (200 ms) in eight of 13 neurons (unpaired *t* test, $p < 0.05$), but the direction of the modulation varied from neuron to neuron (two increased and six decreased). In the population, the drug effect was not statistically significant (paired *t* test, $t_{12} = 0.067$, $p = 0.95$) even when the response to stimulus omission was extracted by subtracting the activity around the time of

the preceding stimulus ($t_{12} = -0.23$, $p = 0.82$).

In contrast to gabazine administration, infusion of a CPP + NBQX compound did not change the variance of baseline activity (Fig. 3D, blue triangles). The CV of inter-spike intervals averaged 0.91 ± 0.17 (SD) before drug administration and 0.99 ± 0.27 during drug administration (paired t test, $t_{12} = -1.33$, $p = 0.21$). For individual neurons, the CV changed significantly in nine out of 13 neurons (6 increased and 3 decreased, one-tailed F test, $p < 0.01$). Again, we did not find any significant drug effect on the width of individual spikes (paired t test, $t_{12} = 0.90$, $p = 0.39$).

Further consideration of drug effects on neuronal activity

The results shown so far indicate that each drug altered different components of neuronal activity during stimulus repetition. To further confirm these findings, additional analyses were performed.

First, since we continued recording until the isolated neuron was lost during drug administration, the pharmacological experiments sometimes lasted long. To ensure that the changes in neuronal activity during drug administration were not due to prolonged recording, we also examined the activity of neurons reported in the previous studies (Ohmae et al., 2013; Uematsu et al., 2017). We selected 17 well isolated neurons that were recorded 50 or more missing oddball trials (ranged from 50–129 trials, mean ± SD, 74.6 ± 24.7) and compared their activity during the first 30 trials with that during the remaining trials. The gain and shift components calculated for these neurons recorded without drug administration averaged 0.97 ± 0.15 (SD) and 5.47 ± 10.76, respectively, which were not significantly different from unity (gain component, one-sample t test, $t_{16} = 0.77$, $p = 0.45$) and zero (shift component, $t_{16} = 2.10$, $p = 0.052$), respectively. In addition, the baseline activity did not alter during the prolonged recording without drug administration (72.4 ± 30.4 spikes/s vs. 75.6 ± 29.3 spikes/s, paired t test, $t_{16} = -2.02$, $p = 0.06$). These results indicate that the changes in neuronal activity during drug infusion described above were not simply due to prolonged recording.

Second, as seen in Figure 2A and D, the firing rate of some neurons greatly increased during gabazine administration, suggesting that neuronal activity might have reached its limit and therefore the modulation of periodic activity decreased. To examine the possibility of a ceiling effect on neuronal activity during drug infusion, we compared the maximum firing rate (measured during 30 ms) within the analysis interval (400–2000 ms from the first stimulus, Experimental procedures) during drug administration with that measured during the 800 ms before to 100 ms after stimulus omission before and during drug administration. Most neurons

normally increase their activity as the number of stimulus repetition (Fig. 2 and Ohmae et al. 2013), but the ceiling effect during drug injection will remove this modulation. However, as shown in Figure 4A, the maximum firing rate during the analysis interval was less than that during the late period in the trial for both gabazine (red circle, paired t test, $t_{14} = -2.53$, $p = 0.02$) and CPP + NBQX (blue circle, $t_{12} = -3.30$, $p = 0.0063$) experiments. Furthermore, the magnitude of periodic firing modulation increased significantly later in the trial (Fig. 4C, paired t test, $t_{14} = -4.00$, $p = 0.0013$ for gabazine, $t_{12} = -3.79$, $p = 0.0026$ for CPP + NBQX). These results indicate that the reduction of the gain component during drug injection seen in Fig. 3C was not due to a ceiling effect on neuronal activity. In addition, as shown in Figure 4B, the peak firing rate (in 30 ms) during the baseline period was much smaller than that measured later during the stimulus repetition (paired t test, $t_{14} = -3.86$, $p = 0.0017$ for gabazine, $t_{12} = -3.83$, $p = 0.0024$ for CPP + NBQX), indicating that the changes in neuronal variability during the baseline period (Fig. 3D) did not reflect a possible ceiling effect.

Finally, we also investigated whether rebound depolarization, a known phenomenon in the cerebellar nucleus (Aizenman and Linden, 1999; Zhang et al., 2004; Zheng and Raman, 2011), plays a role in shaping the firing patterns during stimulus repetition. Specifically, we compared the firing rate during the 100 ms before a long pause (> 100 ms) with that during the subsequent 100 ms, for the interval from 500 ms before to 2000 ms after the first stimulus in sequence. Of the 28 neurons, 15 showed sufficient number of long pauses (> 10) in trials before drug infusion, two of them exhibited a significant increase in firing rate after the pause (paired t test, $p < 0.05$). In the population, the ratio of activity after the pause to that before it averaged 1.03 ± 0.18 (SD, $n = 15$), which was not different from unity (one-sample t test, $t_{14} = 0.66$, $p = 0.52$). These values measured during drug administration were 0.98 ± 0.16 ($n = 6$) and 0.98 ± 0.11 ($n = 11$) in the gabazine and the CPP + NBQX experiments, respectively. Again, the activity after the pause was not significantly enhanced in both experiments (one-sample t test, $t_5 = -0.33$ and $t_{10} = -0.68$, $p > 0.05$). Similar results were obtained when the three spike intervals before and after the pause were used to calculate the rebound activity (Alviña et al., 2008, Hoebeek et al., 2010).

Discussion

We examined the relative contributions of GABAergic and glutamatergic inputs to the neuronal activity in the cerebellar dentate nucleus. When monkeys attempted to detect an omission of isochronously presented visual stimuli, neurons in the posterior part of the dentate nucleus exhibited periodic activity, showing a transient suppression of firing rate followed by a rapid recovery of neuronal activity that peaked around the time of the next stimulus (Fig. 2A and D).

During local application of a selective $GABA_A$ antagonist (gabazine), the amplitude of oscillatory activity decreased, the baseline firing rate increased, and these changes were correlated (Fig. 3A). During infusion of a mixture of glutamate receptor antagonists (NBQX and CPP), the firing modulation for each stimulus clearly decreased in some neurons while the effects were not statistically significant in the population, and the changes in baseline activity varied from neuron to neuron (Fig. 3B). Since the recorded neurons were capable of altering their firing rate beyond the range used in the quantitative analysis, it is unlikely that a ceiling effect influenced the present results (Fig. 4A and B). During both pharmacological manipulations, we only found modulatory changes in neuronal activity; neither the baseline activity nor the periodic firing modulation entirely disappeared. The modulatory effects of drugs were likely because the injected volume was very small in the present study and neurons in the dentate nucleus often extend large dendrites (Uusisaari et al., 2007). Furthermore, previous studies using rodent cerebellar slices have shown that neurons in the cerebellar nuclei exhibit spontaneous firing (Jahnsen, 1986; Aizenman and Linden, 1999; Uusisaari et al., 2007), even when synaptic inputs have been removed (Raman et al., 2000).

We also found that the coefficient of variation of the baseline firing rate decreased during blockade of GABAergic inputs but remained unchanged or even increased during administration of glutamate receptor antagonists (Fig. 3D). Because both drugs did not alter animals' behavior in all but one experiments, the changes in neuronal activity were likely to have resulted from the direct pharmacological effects on the local circuits. These results suggest that the GABAergic signals from the Purkinje cells and/or local inhibitory interneurons may play a major role in both the generation of predictive, periodic neuronal firing and setting the level and variance of baseline activity in the dentate nucleus.

Sources of sensory prediction signals in the deep cerebellar nucleus

Although neurons in the dentate nucleus have been shown to exhibit a transient activity during limb movements (Holdefer and Miller, 2009; Ishikawa et al., 2014), its generation mechanism remains elusive. In addition to the monoaminergic signals from the brainstem, there are three major sources of signals to the deep cerebellar nuclei. The collaterals of climbing fibers provide excitatory inputs of less than a few hertz and it is generally believed that they cannot be the driving signals for movement-related activities in the cerebellar nuclei that need to be controlled on a time scale of tens of milliseconds. However, recent studies have shown that the activity of cerebellar nucleus neurons can be significantly altered when the input of multiple climbing fibers is synchronized (Tang et al., 2019).

More likely to be relevant to the generation of movement signals are the inputs from mossy fibers and Purkinje cells, which are mediated by glutamate and GABA, respectively. Using a similar technique to the present study, Holdefer et al. (2005) demonstrated in monkeys that the movement-related transient activity in the cerebellar dentate nucleus persisted even after local injection of GABA receptor antagonists, suggesting that the direct mossy fiber inputs may play a role. On the other hand, the pervious findings of the post-inhibitory rebound activity in cerebellar slices suggest the possibility that transient inhibition from Purkinje cells may lead a transient activity in the deep cerebellar nucleus (Aizenman and Linden, 1999; Zhang et al., 2004; Zheng and Raman, 2011), although it remains controversial whether this mechanism works *in vivo* (Alviña et al., 2008; Hoebeek et al., 2010). In this study, we failed to find obvious rebound activity, suggesting that the mechanism may not be responsible for the generation of periodic activity during our behavioral task. A recent study comparing the time courses of neuronal activity in Purkinje cells and the dentate nucleus in behaving monkeys showed that the increased activity in Purkinje cells did not precede that in the dentate nucleus in the population (Ishikawa et al., 2014). Instead, the timing of *pauses* of firing in Purkinje cells was similar to the timing of burst firing in the dentate nucleus, suggesting that the release of sustained inhibition exerted from the cerebellar cortex (i.e., disinhibition) might underlie the transient activity in the cerebellar nucleus (Ishikawa et al., 2014). Furthermore, a recent study in the primate cerebro-cerebellum has demonstrated that neuronal activity in the dentate nucleus predicts mossy fiber inputs by tens of milliseconds, suggesting that cerebellar output may serve as a forward model (Tanaka et al., 2019), which may be generated by multiple inputs (Tanaka et al., 2020).

Although our results also suggest a major role for GABAergic inputs in the generation of periodic activity in the dentate nucleus, it should be noted that the prediction signals examined in this study differed from the movement-related burst of activity in two important ways. First, the oscillatory activity during the missing oddball paradigm was observed in the absence of movement, indicating that neuronal activity was sensory-driven in nature. Second, the initial response to each stimulus was a transient *suppression* of firing rate that was followed by a gradual ramp-up of activity. Our previous studies showed that the magnitude of suppressive response was proportional to the time from the previous stimulus, resulting in different time courses of ramping activity that peaked around the time of the next stimulus (Kameda et al., 2019; Figs. 2A and D). These signals may be causally related to temporal prediction, as the detection of stimulus omission was delayed by local inactivation (Ohmae et al., 2013) and facilitated by electrical stimulation (Uematsu et al., 2017), regardless of the direction of eye

movement generated. Since changes in the magnitude of suppressive response are essential for the generation of predictive signals, time-dependent inhibition from the cerebellar cortex may underlie these signals.

Nevertheless, our data also suggest a role for the glutamatergic signals. Changes in the magnitude of periodic activity during infusion of glutamate receptor antagonists were not statistically significant in the population, but three out of 13 neurons showed a significant decrease in the periodic activity (Fig. 3C). Unexpectedly, the blockade of glutamatergic signals sometimes elevated the baseline activity (Fig. 3B), suggesting that the glutamatergic signals may indirectly regulate the firing of recorded neurons. For example, inhibitory interneurons known in the deep cerebellar nuclei (Uusisaari et al., 2007) might mediate the mossy fiber inputs, or alternatively, putative excitatory interneurons might transmit signals from Purkinje cells. Contrary to the gabazine experiments, the alteration of periodic activity and baseline firing rate during CPP+NBQX application did not closely correlate, indicating that different glutamatergic inputs might regulate these parameters. In relation to this, the previous studies in rodents have demonstrated that neurons in the dentate nucleus receive only a little input from the pontine nuclei (Na et al., 2019) but receive strong projections of mossy fiber collaterals from the brainstem (Wu et al., 1999), suggesting that the dentate nucleus might integrate information from different functional modules (Tanaka et al., 2020). Thus, the effects of glutamatergic signals were weaker and less consistent than those of GABAergic signals in our experimental conditions, while they could also contribute to shape the temporally specific predictive signals in the cerebellar nucleus.

Similar to the firing of neurons examined in this study, a transient suppression followed by gradual rebound has been reported in the time course of beta coherence between the auditory cortex and the cerebellum in humans passively listening to an isochronous auditory rhythm (Fujioka et al., 2012). Such representation of periodic sensory events might be prevalent in the brain when keeping rhythms (Matsuyama and Tanaka, 2021). Current results suggest that computations in the cerebellar cortex might be crucial for the generation of these signals. For example, time-specific transient activity or increased synchrony of individual Purkinje cells might play a role. These possibilities are to be tested in future studies.

Possible roles of intrinsic circuits within the cerebellar nucleus

The cerebellar nuclei contain four types of projection neurons and at least two types of interneurons (Sultan et al., 2003, for reviews, see Uusisaari and Knöpfel, 2011; Canto et al., 2016). Because all neurons examined in this study were successfully isolated for tens of minutes

and exhibited high baseline firing rate (on average, 58.7 spikes/s), they were likely to be the largest, glutamatergic projection neurons. Since these neurons receive massive projections directly from Purkinje cells and collaterals of mossy and climbing fibers, local injection of antagonists is expected to primarily block these external inputs. However, as discussed above, some of pharmacological effects might also be attributed to the changes in the internal signals mediated by interneurons. It should be noted that the previous study in cats showed that the mossy fiber projections to the dentate nucleus were less than those to the other cerebellar nuclei (Shinoda et al., 1992), although it remains unclear whether this is also true for the primates that have much extensively evolved dentate nucleus (Kebschull et al., 2020). In the present experiments, individual neurons changed the baseline activity in different directions during local application of glutamate receptor antagonists (Fig. 3B). While the precise projection patterns of small GABAergic and putative glutamatergic (non-GABAergic) interneurons are not known, pharmacological manipulation of these neurons might alter the output signals from the cerebellar nuclei (Uusisaari and De Schutter, 2011).

In relation to this issue, we were interested in the changes in variation of baseline activity during drug application. The decreased variation during blockade of GABAergic inputs (Fig. 3D) suggests that neuronal noise in the output node of the cerebellum might mainly come from the cerebellar cortex. These hypotheses are highly speculative and need to be tested in future studies with cell-type specific manipulation of neuronal activity.

Finally, it is important to point out the limitations of the present study. Although about half of the periodic activity remained after blockade of GABAergic input, we were unable to conclude that the signals from mossy and/or climbing fibers contributed to the remaining activity. The weaker effect of CPP + NBQX than gabazine might be related to the fact that excitatory inputs tend to terminate in the distal part of the dendrite and inhibitory inputs in the proximal part. In addition, as discussed above, our pharmacological technique cannot distinguish between direct external input and signals through interneurons. To resolve these issues, pathway-specific inhibition using optogenetics, which has recently become available in primates (Suzuki et al., 2021), may be helpful in future studies.

Acknowledgements

The authors thank M. Kameda for his help in analyzing data; T. Mori, A. Hironaka and H. Miyaguchi for their assistance with animal care, surgery, and histological procedures; M. Suzuki for her administrative help; M. Takei and M. Kusuzaki for manufacturing equipment; and all lab members for comments and discussions. We are also grateful to A. Nambu, S. Chiken

and Y. Tachibana in the National Institute for Physiological Sciences for providing technical information on manufacturing injectrodes. Animals were provided by the National Bio-Resource Project. This work was supported in part by grants from the Ministry of Education, Culture, Sports, Science and Technology of Japan (25119005, 18H05523, 21H04810) and the Takeda Science Foundation. The authors declare no competing financial interests.

References

Aizenman CD, Linden DJ (1999) Regulation of the rebound depolarization and spontaneous firing patterns of deep nuclear neurons in slices of rat cerebellum. J Neurophysiol 82:1697–1709.

Alviña K, Walter JT, Kohn A, Ellis-Davies G, Khodakhah K (2008) Questioning the role of rebound firing in the cerebellum. Nat Neurosci 11:1256–1258.

Ashmore RC, Sommer MA (2013) Delay activity of saccade-related neurons in the caudal dentate nucleus of the macaque cerebellum. J Neurophysiol 109:2129–2144.

Bares M, Lungu OV, Liu T, Waechter T, Gomez CM, Ashe J (2011) The neural substrate of predictive motor timing in spinocerebellar ataxia. Cerebellum 10:233–244.

Bartolo R, Merchant H (2009) Learning and generalization of time production in humans: Rules of transfer across modalities and interval durations. Exp Brain Res 197:91–100.

Bellebaum C, Daum I, Suchan B (2012) Mechanisms of cerebellar contributions to cognition in humans. Wiley Interdiscip Rev Cogn Sci 3:171–184.

Breska A, Ivry RB (2016) Taxonomies of timing: Where does the cerebellum fit in? Curr Opin Behav Sci 8:282–8.

Canto CB, Witter L, De Zeeuw CI (2016) Whole-cell properties of cerebellar nuclei neurons in vivo. PLoS One 11:1–19.

Cerminara NL, Apps R, Marple-Horvat DE (2009) An internal model of a moving visual target in the lateral cerebellum. J Physiol 587:429–442.

Chabrol FP, Blot A, Mrsic-Flogel TD (2019) Cerebellar contribution to preparatory activity in motor neocortex. Neuron 103:506–519.

Chiken S, Nambu A (2013) High-frequency pallidal stimulation disrupts information flow through the pallidum by GABAergic inhibition. J Neurosci 33:2268–2280.

Comstock DC, Ross JM, Balasubramaniam R (2021) Modality-specific frequency band activity during neural entrainment to auditory and visual rhythms. Eur J Neurosci 54:4649–4669.

E K-H, Chen S-HA, Ho M-HR, Desmond JE (2014) A meta-analysis of cerebellar contributions to higher cognition from PET and fMRI studies. Hum Brain Mapp 35:593–615.

Fortier PA, Kalaska JF, Smith AM (1989) Cerebellar neuronal activity related to whole-arm reaching movements in the monkey. J Neurophysiol 62:198–211.

Fujioka T, Trainor LJ, Large EW, Ross B (2012) Internalized timing of isochronous sounds is represented in neuromagnetic beta oscillations. J Neurosci 32:1791–1802.

Harvey RJ, Porter R, Rawson JA (1979) Discharges of intracerebellar nuclear cells in monkeys. J Physiol 297:559–580.

Heiney SA, Kim J, Augustine GJ, Medina JF (2014) Precise Control of Movement Kinematics by Optogenetic Inhibition of Purkinje Cell Activity. J Neurosci 34:2321–2330.

Hoebeek FE, Witter L, Ruigrok TJH, De Zeeuw CI (2010) Differential olivo-cerebellar cortical control of rebound activity in the cerebellar nuclei. Proc Natl Acad Sci U S A. 107:8410–8415.

Holdefer RN, Houk JC, Miller LE (2005) Movement-related discharge in the cerebellar nuclei persists after local injections of GABA(A) antagonists. J Neurophysiol 93:35–43.

Holdefer RN, Miller LE (2009) Dynamic correspondence between Purkinje cell discharge and forelimb muscle activity during reaching. Brain Res 1295:67–75.

Hove MJ, Fairhurst MT, Kotz SA, Keller PE (2013) Synchronizing with auditory and visual rhythms: An fMRI assessment of modality differences and modality appropriateness. Neuroimage 67:313–321.

Ishikawa T, Tomatsu S, Tsunoda Y, Lee J, Hoffman DS, Kakei S (2014) Releasing dentate nucleus cells from Purkinje cell inhibition generates output from the cerebrocerebellum. PLoS One 9:e108774.

Ivry R, Keele S, Diener H (1988) Dissociation of the lateral and medial cerebellum in movement timing and movement execution. Exp Brain Res 73:167–180.

Jahnsen H (1986) Electrophysiological characteristics of neurones in the guinea-pig deep cerebellar nuclei in vitro. J Physiol 372:129–147.

Kameda M, Ohmae S, Tanaka M (2019) Entrained neuronal activity to periodic visual stimuli in the primate striatum compared with the cerebellum. eLife 8:e48702.

Kebschull JM, Richman EB, Ringach N, Friedmann D, Albarran E, Kolluru SS, Jones RC, Allen WE, Wang Y, Cho SW, Zhou H, Ding JB, Chang HY, Deisseroth K, Quake SR, Luo L (2020) Cerebellar nuclei evolved by repeatedly duplicating a conserved cell-type set. Science 370:eabd5059.

Kita H, Nambu A, Kaneda K, Tachibana Y, Takada M (2004) Role of ionotropic glutamatergic and GABAergic inputs on the firing activity of neurons in the external pallidum in awake monkeys. J Neurophysiol 92:3069–3084.

Kotz S a, Stockert A, Schwartze M (2014) Cerebellum, temporal predictability and the updating of a mental model. Philos Trans R Soc Lond B Biol Sci 369:20130403.

Koziol LF, Budding D, Andreasen N, D'Arrigo S, Bulgheroni S, Imamizu H, Ito M, Manto M, Marvel C, Parker K, Pezzulo G, Ramnani N, Riva D, Schmahmann J, Vandervert L, Yamazaki T (2014) Consensus Paper: The Cerebellum's Role in Movement and Cognition. Cerebellum 13:151–177.

Lee SM, Peltsch A, Kilmade M, Brien DC, Coe BC, Johnsrude IS, Munoz DP (2016) Neural Correlates of Predictive Saccades. J Cogn Neurosci 28:1210–1227.

Matsuyama K, Tanaka M (2021) Temporal prediction signals for periodic sensory events in the primate central thalamus. J Neurosci 41:1917–1927.

Matsuda S, Matsumoto H, Furubayashi T, Hanajima R, Tsuji S, Ugawa Y, Terao Y (2015) The 3-second rule in hereditary pure cerebellar ataxia: a synchronized tapping study. PLoS One 10:e0118592.

Merchant H, Zarco W, Perez O, Prado L, Bartolo R (2011) Measuring time with different neural chronometers during a synchronization-continuation task. Proc Natl Acad Sci 108:19784–19789.

Na J, Sugihara I, Shinoda Y (2019) The entire trajectories of single pontocerebellar axons and their lobular and longitudinal terminal distribution patterns in multiple aldolase C-positive compartments of the rat cerebellar cortex. J Comp Neurol 527:2488–2511.

Nashef A, Cohen O, Harel R, Israel Z, Prut Y (2019) Reversible block of cerebellar outflow reveals cortical circuitry for motor coordination. Cell Rep 27:2608–2619.

Ohmae S, Kunimatsu J, Tanaka M (2017) Cerebellar roles in self-timing for sub- and supra-second intervals. J Neurosci 37:2221–2216.

Ohmae S, Tanaka M (2016) Two different mechanisms for the detection of stimulus omission. Sci Rep 6:20615.

Ohmae S, Uematsu A, Tanaka M (2013) Temporally Specific Sensory Signals for the Detection of Stimulus Omission in the Primate Deep Cerebellar Nuclei. J Neurosci 33:15432–15441.

Perrett SP, Ruiz BP, Mauk MD (1993) Cerebellar cortex lesions disrupt learning-dependent timing of conditioned eyelid responses. J Neurosci 13:1708–1718.

Person AL, Raman IM (2012) Purkinje neuron synchrony elicits time-locked spiking in the cerebellar nuclei. Nature 481:502–505.

Raman IM, Gustafson AE, Padgett D (2000) Ionic currents and spontaneous firing in neurons isolated from the cerebellar nuclei. J Neurosci 20:9004–9016.

Ramnani N (2006) The primate cortico-cerebellar system: anatomy and function. Nat Rev Neurosci 7:511–522.

Roth MJ, Synofzik M, Lindner A (2013) The cerebellum optimizes perceptual predictions about external sensory events. Curr Biol 23:930–935.

Sakai K, Hikosaka O, Miyauchi S, Takino R, Tamada T, Iwata NK, Nielsen M (1999) Neural representation of a rhythm depends on its interval ratio. J Neurosci 19:10074–10081.

Shadmehr R (2017) Learning to Predict and Control the Physics of Our Movements. J Neurosci 37:1663–1671.

Shinoda Y, Sugiuchi Y, Futami T, Izawa R (1992) Axon collaterals of mossy fibers from the pontine nucleus in the cerebellar dentate nucleus. J Neurophysiol 67:547–560.

Sokolov AA, Miall RC, Ivry RB (2017) The cerebellum: Adaptive prediction for movement and cognition. Trends Cogn Sci 21:313–332.

Spencer RMC, Zelaznik HN, Diedrichsen J, Ivry RB (2003) Disrupted timing of discontinuous but not continuous movements by cerebellar lesions. Science 300:1437–1439.

Steuber V, Schultheiss NW, Silver RA, De Schutter E, Jaeger D (2011) Determinants of synaptic integration and heterogeneity in rebound firing explored with data-driven models of deep cerebellar nucleus cells. J Comput Neurosci 30:633–658.

Stoodley CJ, Schmahmann JD (2009) Functional topography in the human cerebellum: a meta-analysis of neuroimaging studies. Neuroimage 44:489–501.

Strick PL, Dum RP, Fiez JA (2009) Cerebellum and nonmotor function. Annu Rev Neurosci 32:413–434.

Sultan F, Czubayko U, Thier P (2003) Morphological classification of the rat lateral cerebellar nuclear neurons by principal component analysis. J Comp Neurol 455:139–155.

Suzuki TW, Inoue KI, Takada M, Tanaka M (2021) Effects of optogenetic suppression of cortical input on primate thalamic neuronal activity during goal-directed behavior. eNeuro 8:ENEURO.0511-20.2021.

Tanaka H, Ishikawa T, Kakei S (2019) Neural evidence of the cerebellum as a state predictor. Cerebellum 18:349–371.

Tanaka H, Ishikawa T, Lee J, Kakei S (2020) The cerebro-cerebellum as a locus of forward model: a review. Front Syst Neurosci 14:19.

Tanaka M, Kunimatsu J, Suzuki TW, Kameda M, Ohmae S, Uematsu A, Takeya R (2021) Roles of the cerebellum in motor preparation and prediction of timing. Neuroscience 462:220–234.

Tachibana Y, Kita H, Chiken S, Takada M, Nambu A (2008) Motor cortical control of internal pallidal activity through glutamatergic and GABAergic inputs in awake monkeys. Eur J Neurosci 27:238–253.

Tang T, Blenkinsop TA, Lang EJ (2019) Complex spike synchrony dependent modulation of rat deep cerebellar nuclear activity. Elife 8:1–24.

Teki S, Griffiths TD (2016) Brain bases of working memory for time intervals in rhythmic sequences. Front Neurosci 10:1–13.

Thach TW, Goodkin HP, Keating JG (1992) the Cerebellum and the Adaptive Coordination. Annu Rev Neurosci 15:403–442.

Uematsu A, Ohmae S, Tanaka M (2017) Facilitation of temporal prediction by electrical stimulation to the primate cerebellar nuclei. Neuroscience 346:190–196.

Uusisaari M, Obata K, Knöpfel T (2007) Morphological and electrophysiological properties of GABAergic and non-GABAergic cells in the deep cerebellar nuclei. J Neurophysiol 97:901–911.

Uusisaari M, De Schutter E (2011) The mysterious microcircuitry of the cerebellar nuclei. J Physiol 589:3441–3457.

Uusisaari M, Knöpfel T (2011) Functional classification of neurons in the mouse lateral cerebellar nuclei. Cerebellum 10:637–646.

van Kan PL, Gibson AR, Houk JC (1993) Movement-related inputs to intermediate cerebellum of the monkey. J Neurophysiol 69:74–94.

Wolpert DM, Miall RC, Kawato M (1998) Internal models in the cerebellum. Trends Cogn Sci 2:338–347.

Wu HS, Sugihara I, Shinoda Y (1999) Projection patterns of single mossy fibers originating from the lateral reticular nucleus in the rat cerebellar cortex and nuclei. J Comp Neurol 411:97–118.

Zhang W, Shin JH, Linden DJ (2004) Persistent changes in the intrinsic excitability of rat deep cerebellar nuclear neurones induced by EPSP or IPSP bursts. J Physiol 561:703–719.

Zheng N, Raman IM (2011) Prolonged postinhibitory rebound firing in the cerebellar nuclei mediated by group I metabotropic glutamate receptor potentiation of L-type calcium currents. J Neurosci 31:10283–10292.

Figure legends

Figure 1. (A) Sequence of events in the missing oddball paradigm. During central fixation, a saccade target appeared either left or right of the fixation point (FP). Then a brief visual stimulus (35 ms) surrounding the FP was repeatedly presented with an interstimulus interval of 400 ms. After a random 2000–4800 ms period, one stimulus in the series was omitted, and monkeys made a saccade to the target. (B) Recording sites reconstructed from histological sections in monkey Z. Labels indicate the posterior locations of coronal sections (in millimeters) relative to the interaural line. DN, dentate nucleus; IA, anterior interposed nucleus; IP, posterior interposed nucleus.

Figure 2. Effects of drug administration on example neurons. (A) Effects of GABA receptor antagonist (gabazine). Each panel shows neuronal activity and eye position aligned with either the first stimulus in the sequence or stimulus omission. Black and red traces represent the data obtained before and during gabazine infusion, respectively. Rasters are plotted for every third spike for clarity. (B) Sample spike waveforms before (black) and during (red) drug application for the neuron shown in (A). Scale bar denotes 200 μs. (C) Time courses of neuronal activity 800 to 2000 ms after the first stimulus before and during gabazine administration for the other two neurons. (D) An example neuron activity with local infusion of glutamate receptor antagonists (a mixture of CPP and NBQX). Black and blue traces indicate the data obtained before and during drug application, respectively. (E) Spike waveforms before (black) and during (blue) drug infusion. (F) The spike density profiles for the other two neurons.

Figure 3. Summary of 15 gabazine and 13 CPP+NBQX experiments. (A) Comparison of the gain and shift components measured from the spike density profiles (400–2000 ms after the first stimulus) before and during drug infusion. Red and blue symbols indicate gabazine and CPP+NBQX experiments, respectively. Bull's eyes denote the representative data shown in Figure 2A and D. (B) Comparison of different measures of the changes in baseline activity. Δ baseline is the difference in the mean firing rates during 500 ms before the first stimulus onset. (C) Histograms of gain components for different drugs. Filled bars indicate data where a significant drug effect was observed by bootstrap method (1000 iterations, $p < 0.05$). (D) Comparison of coefficient of variation (CV) in baseline activity between trials before and during drug administration.

Figure 4. Peak firing rate and the magnitude of activity modulation at different epochs. (A) Comparison of peak firing rates (30 ms interval) measured within the analysis interval (400–

2000 ms after the first stimulus, *Early*) during drug administration with those measured during the later period in the trial (800 ms before to 100 ms after stimulus omission, *Late*). (B) Comparison of peak activity between the late and the baseline periods (500 ms before the first stimulus) during drug administration. (C) Comparison of the magnitude of activity modulation during the early and later periods during the stimulus repetition. In all panels, the color of symbols indicates different drugs.

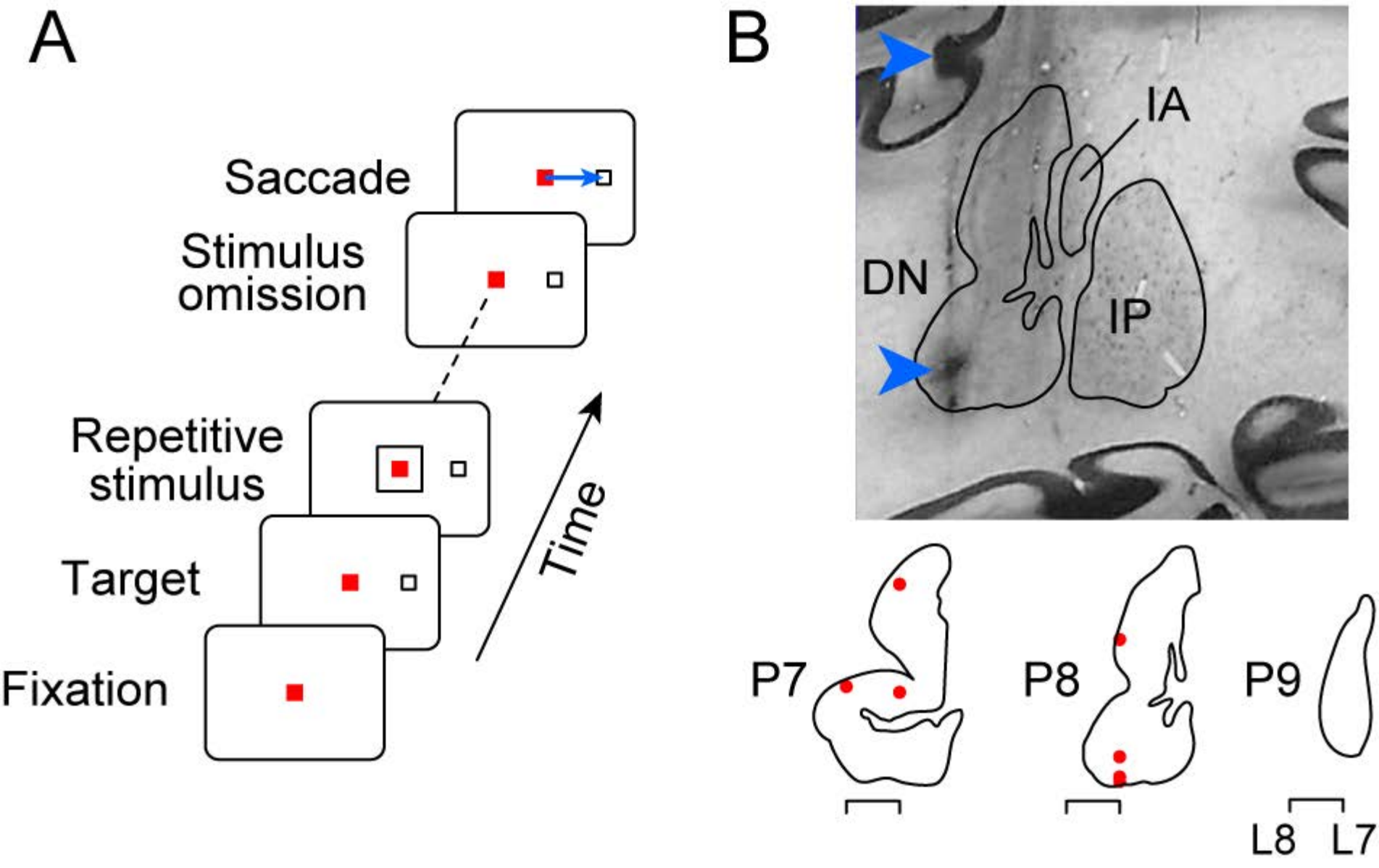
A
Saccade
Stimulus omission
Repetitive stimulus
Target
Fixation
Time
B
IA
DN
IP
P7
P8
P9
L8
L7

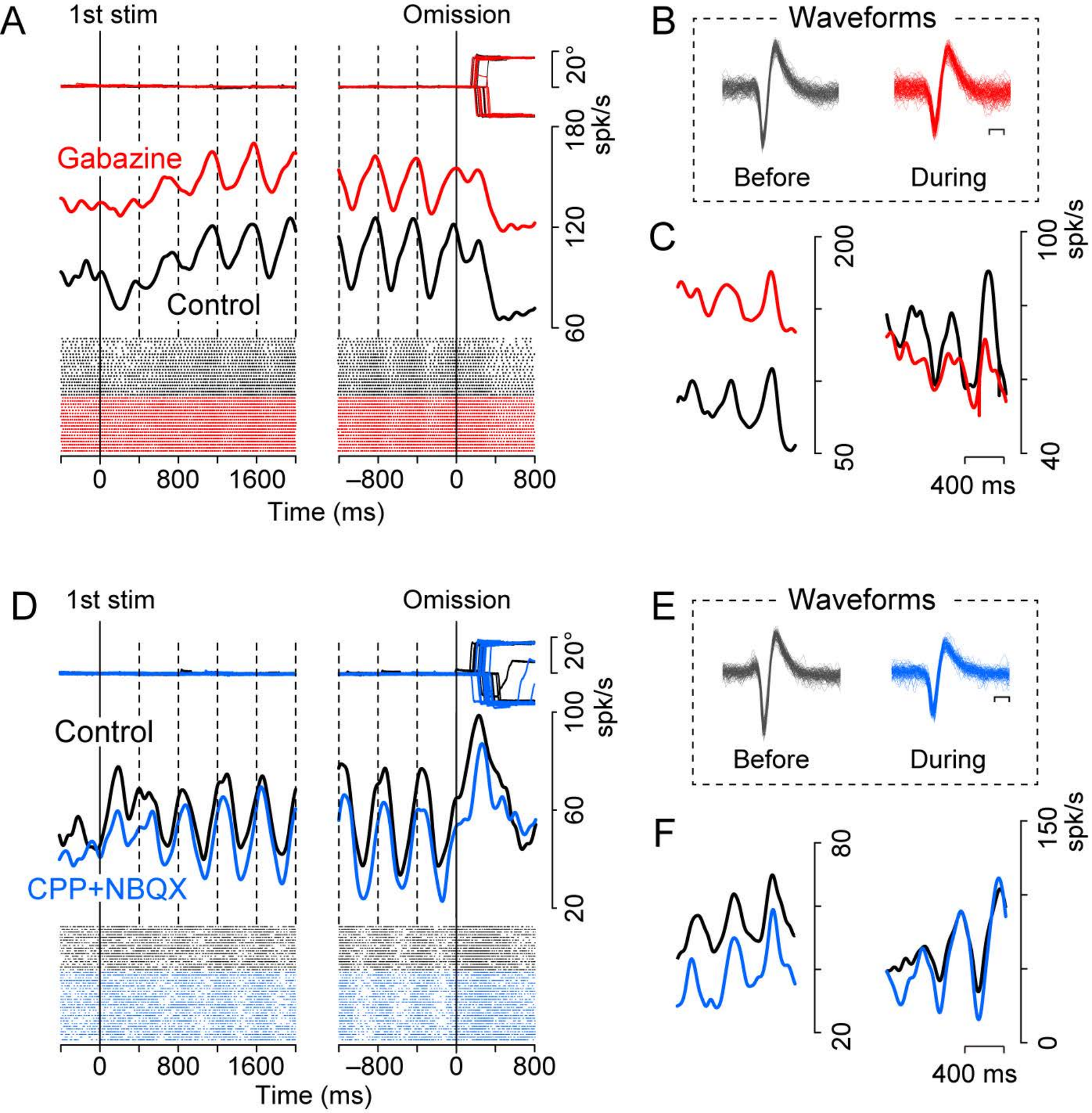
A
1st stim
Omission
Gabazine
Control
20°
180
120
60
spk/s
0
800
1600
–800
0
800
Time (ms)
B
Waveforms
Before
During
C
200
50
100
40
spk/s
400 ms
D
1st stim
Omission
Control
CPP+NBQX
20°
100
60
20
spk/s
0
800
1600
–800
0
800
Time (ms)
E
Waveforms
Before
During
F
80
20
150
0
spk/s
400 ms

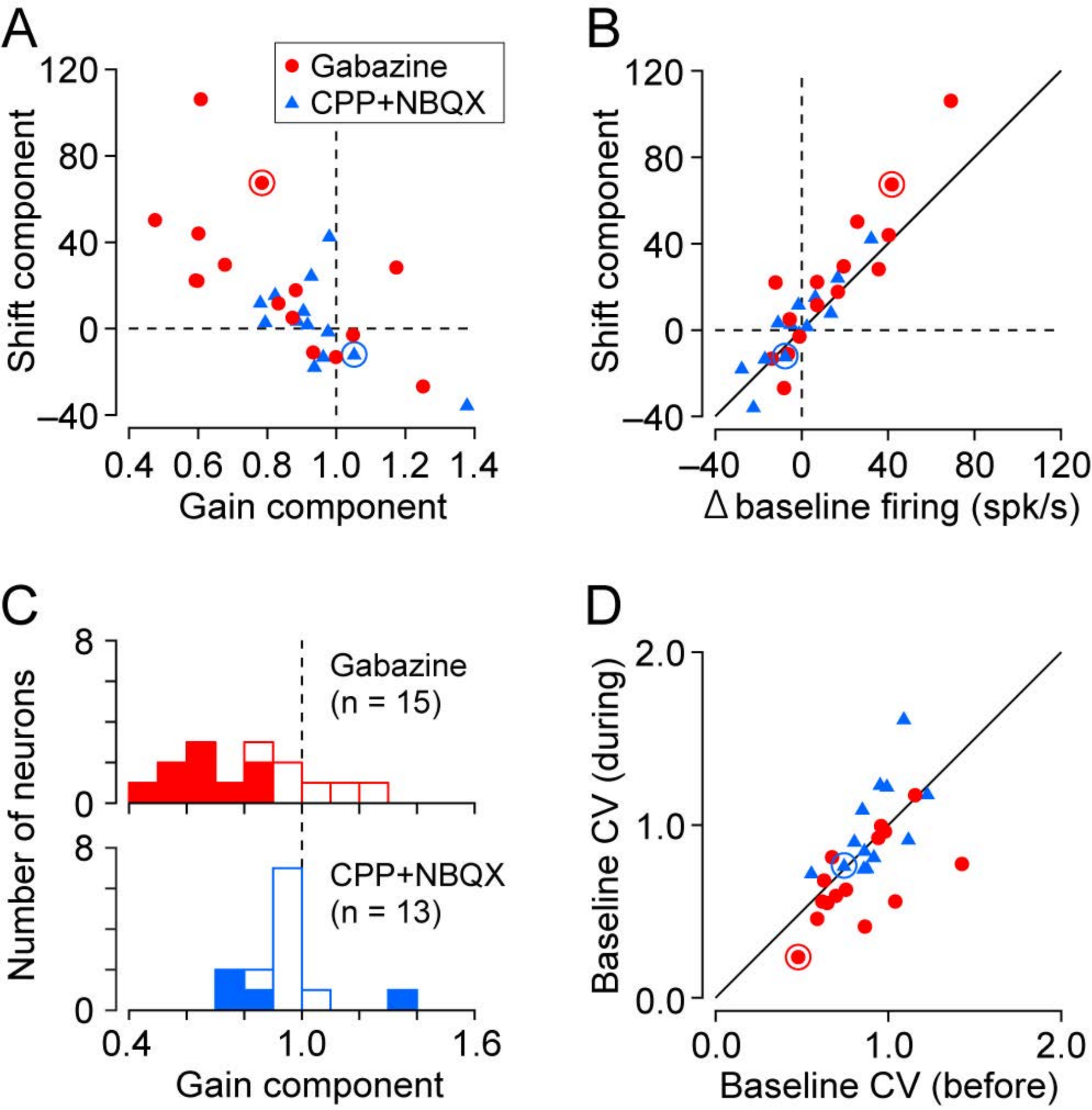
A
Gabazine
CPP+NBQX
120
80
40
0
–40
Shift component
0.4
0.6
0.8
1.0
1.2
1.4
Gain component
B
120
80
40
0
–40
Shift component
–40
0
40
80
120
Δ baseline firing (spk/s)
C
8
0
Gabazine
(n = 15)
8
0
CPP+NBQX
(n = 13)
Number of neurons
0.4
1.0
1.6
Gain component
D
2.0
1.0
0.0
Baseline CV (during)
0.0
1.0
2.0
Baseline CV (before)

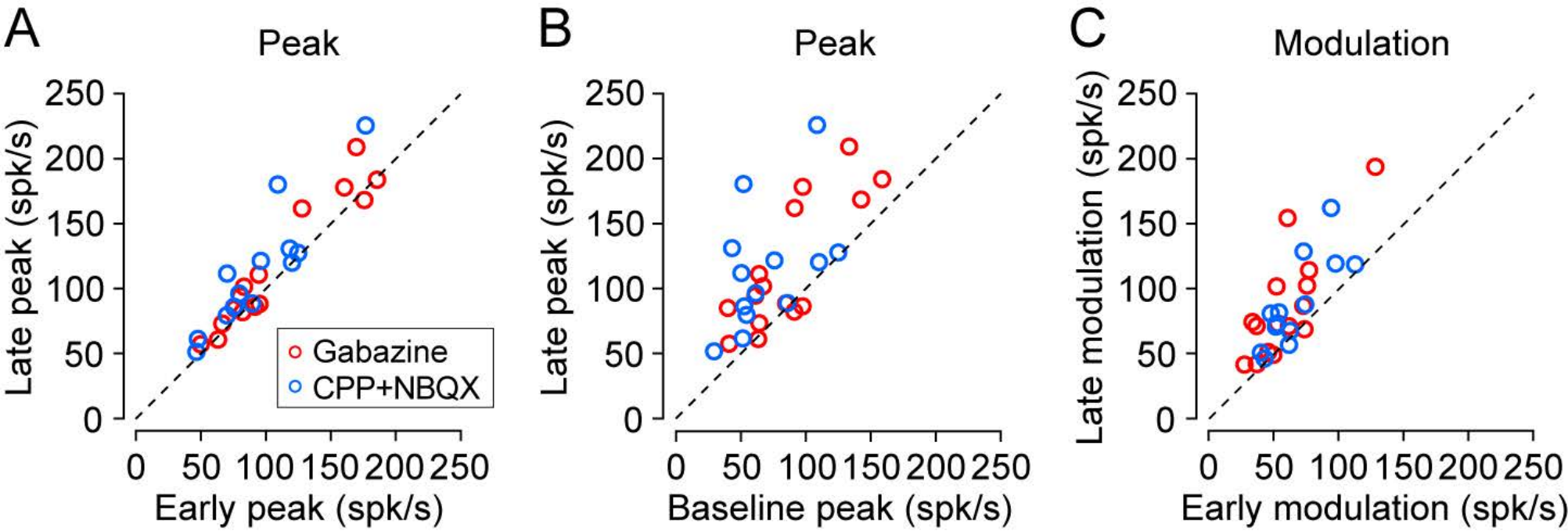
A
Peak
Late peak (spk/s)
Early peak (spk/s)
Gabazine
CPP+NBQX
B
Peak
Late peak (spk/s)
Baseline peak (spk/s)
C
Modulation
Late modulation (spk/s)
Early modulation (spk/s)
0
50
100
150
200
250